Brief Note

Large post-buckling of heavy tapered elastica cantilevers and its asymptotic analysis

C. Y. WANG

Departments of Mathematics and Mechanical Engineering
Michigan State University
East Lansing, MI 48824, U.S.A.
e-mail: cywang@mth.msu.edu

COMPLETE CHARACTERISTICS OF THE DEFORMATIONS of a tapered cantilever due to self weight are studied. Explicit stability criteria for pointy tapered columns and numerical results for the blunt columns are given. Asymptotic formulas for large deformations are derived, and the results compare well with those from numerical integration. It is found that the deformation depends heavily on a non-dimensional gravity parameter, the degree of taper and the cross sectional shape of the cantilever.

Key words: elastica, taper, heavy, cantilever.

1. Introduction

THE ELASTIC CANTILEVER is a structural element that models poles, masts, antennas and mechanisms. A very slender or highly flexible cantilever, or elastica, can admit large reversible deformations. The theory for the elastica was first formulated by EULER [1], who defined the elastica as a slender rod whose curvature at any point is proportional to the local moment experienced. If the deformation is due to self weight, it is called a heavy elastica. Note that large non-negligible body forces, which is equivalent to self weight, can be created by an acceleration of the system. GREENHILL [2] first correctly found the stability criteria for a standing uniform heavy cantilever. Various aspects of the uniform heavy elastica cantilever have been reported previously, e.g. [3–9].

Less work has been done on the non-uniform heavy cantilever. The stability for the vertical pointy heavy cantilever, i.e. the tip tapered into a sharp point, was solved by DINNIK [10] in terms of Bessel functions. The same problem was investigated by STUART [11] for qualitative behaviors. Non-unique solutions for the inclined pointy tapered cantilever were also reported [12, 13]. There exist results on blunt (non-pointy) tapered cantilevers with distributed loads [14–16], but these sources only considered small to moderate post-buckling cases.

Due to the advancements in flexible materials, large deformations are becoming more important. For tapered heavy elastica, the existing literature is limited to a few special geometries, and none for large deformations. This is probably due to the incurred stiffness of the governing equation, such that conventional numerical integration becomes inaccurate. The present paper considers the large deformations of general tapered heavy elastica cantilevers. The cantilevers may have different cross sectional shapes and need not be pointy. Since the governing equation becomes singular for large deformations, a matched asymptotic perturbation method will be used. The results are compared to those from direct numerical integration.

2. Formulation

Figure 1 shows a cantilever of length L subjected to its own weight. The angle between the gravity direction and the base inclination is γ. When $\gamma = 0$ the undeformed cantilever is a vertical column, and when $\gamma = \pi/2$ it is a horizontal cantilever. Let s' be the arc length from the base and θ be the local inclination after deformation. A moment balance on an elemental length gives

$$(2.1) \qquad\qquad M' = M' + dM' + P' \sin\theta \, ds',$$

where M' is the local moment and P' is the weight from s' to the tip

$$(2.2) \qquad\qquad P' = \int_{s'}^{L} \rho g \, ds'.$$

Here ρ is the mass per length, which for non-uniform cantilevers is a function of s', and g is the gravitational acceleration. Euler's constitutive relation is

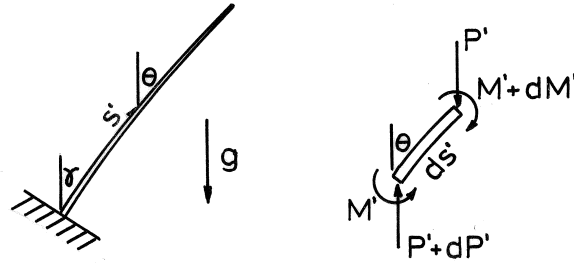$$(2.3) \qquad\qquad M' = EI \frac{d\theta}{ds'}.$$

Fig. 1. The tapered cantilever under self weight and an elemental segment.

Here EI is the flexural rigidity, which is also a function of s'. Eqs. (2.1)–(2.3) give

$$(2.4) \qquad \frac{d}{ds'}\left(EI\frac{d\theta}{ds'}\right) + g\int_{s'}^{L}\rho\,ds'\sin\theta = 0.$$

Normalize all lengths by L and drop primes. Let EI_0 be the flexural rigidity and ρ_0 be the density at the larger fixed (base) end, and

$$(2.5) \qquad EI = EI_0 l(s), \qquad \rho = \rho_0 r(s).$$

Eq. (2.4) becomes

$$(2.6) \qquad \frac{d}{ds}\left(l(s)\frac{d\theta}{ds}\right) + \beta\int_{s}^{1} r(s)ds\sin\theta = 0,$$

where $\beta = \rho_0 g L^3/EI_0$ is an important non-dimensional parameter characterizing gravity. The boundary conditions for the cantilever are

$$(2.7) \qquad \theta(0) = \gamma,$$

$$(2.8) \qquad \frac{d\theta}{ds}(1) = 0.$$

After $\theta(s)$ is obtained, the shape of the deformed cantilever can be determined from the Cartesian coordinates

$$(2.9) \qquad x = \int_{0}^{s}\cos\theta\,ds, \qquad y = \int_{0}^{s}\sin\theta\,ds.$$

For linearly tapered cantilevers, the rigidity function $l(s)$ and density function $r(s)$ can be expressed as

$$(2.10) \qquad l(s) = (1-cs)^m, \qquad r(s) = (1-cs)^n,$$

where $0 \le c \le 1$ and $m, n \ge 0$ are constants. The cantilever is uniform if $c = 0$ or $m = n = 0$. The cantilever is pointy when $c = 1$, which is the case considered by most previous authors.

The exponents m and n govern the cross section properties. Fig. 2a shows the case where the cross section is similar (e.g. circular) and the diameter tapers linearly. In this acse $m = 4$ and $n = 2$. Figure 2b shows the case when the thickness is constant but the width tapers linearly. If the cantilever bends in the width direction, along the axis A-A, then $m = 3$ and $n = 1$. If it bends in the
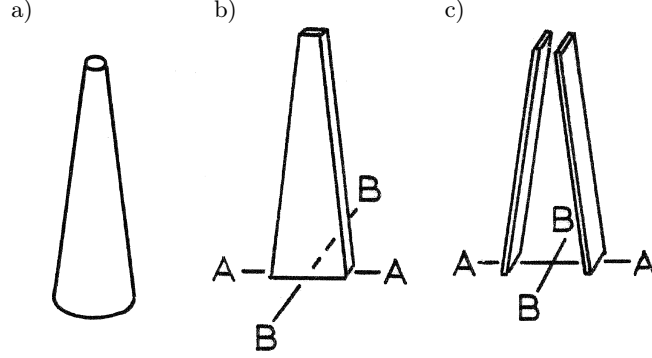
FIG. 2. Exaggerated tapered cantilever shapes.

thickness direction, along the axis B-B, then $m = 1$ and $n = 1$. Figure 2c shows a composite cantilever which is composed of two slats held together by a filling or webbing of negligible mass. If it bends along the axis A-A, then $m = 2$ and $n = 0$. If it bends along the axis B-B, then $m = 0$ and $n = 0$, same as the uniform case. HWANG and YEH [12] studied only the $m = 4$, $n = 2$ case.

3. The stability problem

The stability problem is relevant for the vertically standing cantilever or column ($\gamma = 0$), where the column would not buckle until a critical β value (β_c) is reached. Exact stability criteria can be derived only for the pointy case ($c = 1$). Following DINNIK [10] we set $\xi = 1 - s$ and Eqs. (2.6) and (2.10) become

$$(3.1) \qquad \xi^2 \frac{d^2\theta}{d\xi^2} + m\xi \frac{d\theta}{d\xi} + \frac{\beta}{(n+1)} \xi^{3-m+n}\theta = 0.$$

The solution can be expressed in terms of Bessel functions J (e.g. [17])

$$(3.2) \qquad \theta \sim \xi^{(1-m)/2} J_{\pm|\frac{1-m}{3+n-m}|}\left(\sqrt{\frac{\beta}{n+1}} \left| \frac{2}{3+n-m} \right| \xi^{(3+n-m)/2} \right).$$

Since the angle θ is finite at the tip at $\xi = 0$, we can discard the unbounded solution in Eq. (3.2). Eq. (2.7) gives $\theta = 0$ at the base at $\xi = 1$. Thus the explicit stability criteria are

$$(3.3) \qquad J_3(2\sqrt{\beta/3}) = 0 \qquad \text{for } m = 4, \, n = 2,$$

$$(3.4) \qquad J_2(2\sqrt{\beta/2}) = 0 \qquad \text{for } m = 3, \, n = 1,$$

(3.5) $$J_1(2\sqrt{\beta}) = 0 \qquad \text{for } m = 2,\ n = 0,$$

(3.6) $$J_0(2\sqrt{\beta/2}/3) = 0 \qquad \text{for } m = 1,\ n = 1.$$

For the uniform column, $m = n = 0$ and any c, the criterion is

(3.7) $$J_{-1/3}(2\sqrt{\beta}/3) = 0.$$

Form Eqs. (3.3)–(3.6) we obtain the critical loads $\beta_c = 30.5298, 13.1873, 3.67049,$ 26.0243 respectively, while DINNIK [10] found 30.6, 13.1, 3.67, 26.0, and HWANG and YEH [12], who only studied the $m = 4$, $n = 2$ case, found 30.5295.

However, most cantilevers are not pointy, but blunt at the tip. Exact criteria do not exist for the non pointy column ($c \neq 1$). Linearizing Eq. (2.6) gives

(3.8) $$\frac{d}{ds}\left((1-cs)^m \frac{d\theta}{ds}\right) + \beta \frac{(1-cs)^{n+1} - (1-c)^{n+1}}{c(n+1)}\theta = 0.$$

We guess β and set

(3.9) $$\theta(0) = 0, \qquad \frac{d\theta}{ds}(0) = 1.$$

Eq. (3.8) is then integrated numerically as an initial value problem. At $s = 1$ we check if Eq. (2.8) is satisfied. Using one-parameter shooting we obtain the results shown in Table 1. For $c = 0$, or the uniform column, $\beta_c = 7.83735$ from Eq. (3.7) for all m and n. For $c = 1$, the results of our numerical method agrees with the exact values from Eqs. (3.3)–(3.6). Only the lowest root is β_c, higher buckling modes exist, but are physically unimportant.

Table 1. Critical loads β_c for various tapers.

m,n	$c = 0.1$	0.2	0.3	0.4	0.5	0.6	0.7	0.8	0.9	1
4,2	8.4144	9.0887	9.8887	10.856	12.054	13.584	15.627	18.527	23.029	30.530
3,1	7.9477	8.0762	8.2281	8.4115	8.6391	8.9319	9.3286	9.9112	10.897	13.187
2,0	7.5035	7.1617	6.8105	6.4481	6.0718	5.6779	5.2606	4.8097	4.3039	3.6705
1,1	8.3047	8.8531	9.5069	10.301	11.289	12.553	14.236	16.592	20.133	26.024

Note the critical loads increase with taper c, except for the $m = 2$, $n = 0$ case.

4. Asymptotic analysis

An asymptotic solution is possible for large deformations caused by large β. We shall use the matched asymptotic perturbation method. Let

(4.1) $$\beta = \frac{1}{\varepsilon^2} \gg 1.$$

Eq. (2.6) shows the interior solution is $\theta = k\pi$. Choose $k = 1$ for the first mode. In the boundary layer set

(4.2) $$s = \varepsilon t, \qquad \theta = \theta_0(t) + \varepsilon\theta_1(t) + \cdots .$$

After some work, the zeroth order equation is $c \neq 0$ or 1)

(4.3) $$\frac{d^2\theta_0}{dt^2} + b\sin\theta_0 = 0, \qquad b = \frac{1 - (1 - c)^{n+1}}{c(n + 1)}$$

with the boundary conditions

(4.4) $$\theta_0(0) = \gamma, \qquad \theta_0(\infty) = \pi.$$

Multiply Eq. (4.3) by $d\theta_0/dt$ and integrate. Using the boundary conditions the solution is found to be

(4.5) $$\theta_0 = \pi - 4\tan^{-1}[he^{-\sqrt{b}t}], \qquad h = \frac{1}{\tan[(\gamma + \pi)/4]}.$$

The first order equation is

(4.6) $$\frac{d^2\theta_1}{dt^2} + b\theta_1\sin\theta_0 = cm\frac{d}{dt}\left(t\frac{d\theta_0}{dt}\right) + t\sin\theta_0$$

$$= cm\left[2\sqrt{b}\cos\left(\frac{\theta_0}{2}\right) - bt\sin\theta_0\right] + t\sin\theta_0.$$

Eq. (4.6) although linear, is still formidable. However, we are fortunate to obtain an exact solution as follows. Let

(4.7) $$u = he^{-\sqrt{b}t}, \qquad t = \frac{-1}{\sqrt{b}}\ln\left(\frac{u}{h}\right).$$

From Eq. (4.5) one can show

(4.8) $$\sin\theta_0 = \frac{4u(1 - u^2)}{(1 + u^2)^2}, \qquad \cos\left(\frac{\theta_0}{2}\right) = \frac{2u}{1 + u^2}.$$

We further set

(4.9) $$\theta_1 = \frac{cm}{\sqrt{b}}H_1(u) + \frac{1}{b\sqrt{b}}H_2(u).$$

Eq. (4.6) gives

(4.10) $$u\frac{d}{du}\left(u\frac{dH_1}{du}\right) - \frac{(u^4 - 6u^2 + 1)}{(1 + u^2)^2}H_1 = \frac{4u}{(1 + u^2)} + \frac{4u(1 - u^2)}{(1 + u^2)^2}\ln\left(\frac{u}{h}\right),$$

(4.11) $$u\frac{d}{du}\left(u\frac{dH_2}{du}\right) - \frac{(u^4 - 6u^2 + 1)}{(1 + u^2)^2}H_2 = -\frac{4u(1 - u^2)}{(1 + u^2)^2}\ln\left(\frac{u}{h}\right).$$

The solution satisfying $H_1(0) = 0$, $H_1(h) = 0$ is

$$(4.12) \qquad H_1 = \frac{u(u^2 - h^2) + 2u(\ln^2 h - \ln^2 u) + 2u\ln(u/h)(1 + 2\ln u)}{2(1 + u^2)}.$$

The solution satisfying $H_2(0) = 0$, $H_2(h) = 0$ is

$$(4.13) \qquad H_2 = \frac{u(u^2 - h^2) - 2u(\ln^2 h - \ln^2 u) + 2u\ln(u/h)(1 - 2\ln u)}{2(1 + u^2)}.$$

We find

$$(4.14) \qquad \frac{dH_1}{du}(h) = 1, \qquad \frac{dH_2}{du}(h) = 1.$$

Note that H_1 and H_2 are universal functions in the sense that they are independent of the cantilever geometry parameters c, b, m,n. These functions are plotted in Fig. 3 for $\gamma = 0$ or $h = 1$.

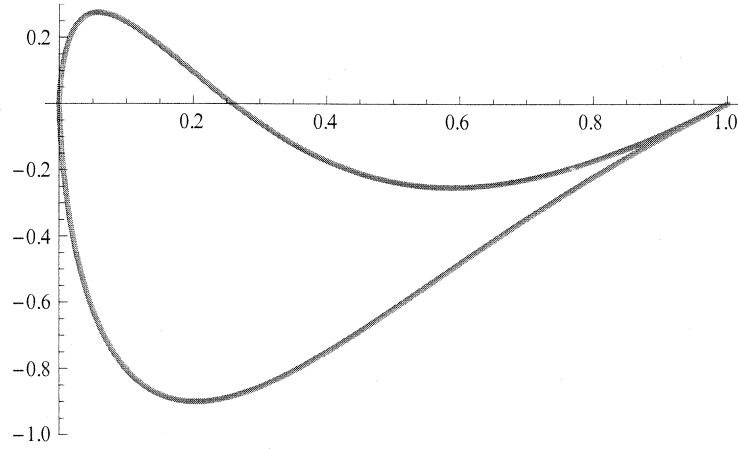

FIG. 3. The universal functions for $h=1$. Top: $H_1(u)$, bottom: $H_2(u)$.

The normalized moment experienced at the base is

$$(4.15) \qquad M_0 = \frac{d\theta}{ds}(0) = \frac{1}{\varepsilon}\left[\frac{d\theta_0}{dt}(0) + \varepsilon\frac{d\theta_1}{dt}(0) + \cdots\right]$$

$$= 2\sqrt{\beta b}\cos\left(\frac{\gamma}{2}\right) - \sqrt{b}h\left[\frac{cm}{\sqrt{b}}\frac{dH_1}{du}(h) + \frac{1}{b\sqrt{b}}\frac{dH_2}{du}(h)\right] + \cdots$$

$$= 2\sqrt{\beta b}\cos\left(\frac{\gamma}{2}\right) - h\left(cm + \frac{1}{b}\right) + O(\beta^{-1/2}).$$

5. Numerical results

Numerical integration is needed for general post-buckling. If $c \neq 0$ or 1 Eqs. (2.6), (2.10) give

$$(5.1) \qquad \frac{d}{ds}\left((1-cs)^m \frac{d\theta}{ds}\right) + \beta \frac{(1-cs)^{n+1} - (1-c)^{n+1}}{c(n+1)} \sin\theta = 0.$$

Guided by Eq. (34) guess $M_0 = d\theta/ds(0)$. Together with $\theta(0) = \gamma$, Eq. (5.1) is integrated by a Runge–Kutta algorithm and we check whether $d\theta/ds(1) = 0$. Using shooting, the following results are obtained.

Table 2 shows the results for the standing cantilever (column) where $\gamma = 0$. The zero entries are when the column is stable with no deformation. Numerical integration suffers from stiffness problems and becomes inaccurate for $\beta > 100$. However, our asymptotic approximations become more accurate as β becomes larger. Since Eq. (5.1) is singular for $c = 1$, we used $c = 0.999$ in our numerical computation.

Table 2a. Base moment M_0 for $m = 4$, $n = 2$ case, $\gamma = 0$.
Values in parentheses are from Eq. (4.15).

$\beta \backslash c$	0.1	0.3	0.5	0.7	0.9	0.999
10	2.4835	0.4820	0	0	0	0
20	6.3809	4.5885	2.8896	1.3056	0	0
50	11.731 (11.93)	9.3659 (9.51)	7.0705 (7.09)	4.8703 (4.67)	2.8038 (2.30)	1.8505 (1.18)
100	17.384 (17.50)	14.436 (14.52)	11.565 (11.56)	8.8028 (8.66)	6.2053 (5.86)	5.0160 (4.56)
200	25.30 (25.38)	21.55 (21.60)	17.90 (17.89)	14.40 (14.29)	11.14 (10.90)	9.66 (9.35)

Table 2b. Base moment M_0 for $m = 3$, $n = 1$ case, $\gamma = 0$.
Values in parentheses are from Eq. (4.15).

$\beta \backslash c$	0.1	0.3	0.5	0.7	0.9	0.999
10	2.9546	2.2594	1.5451	0.7683	0	0
20	6.7784	5.7101	4.6143	3.4734	2.2376	1.5305
50	12.234 (12.43)	10.800 (10.96)	9.3140 (9.41)	7.7515 (7.76)	6.0649 (5.97)	5.1505 (5.01)
100	18.025 (18.14)	16.267 (16.36)	14.429 (14.49)	12.485 (12.49)	10.383 (10.31)	9.2536 (9.15)
200	26.14 (26.22)	23.94 (24.00)	21.63 (21.66)	19.17 (19.17)	16.51 (16.46)	15.09 (15.02)

Table 2c. Base moment M_0 for $m = 2$, $n = 0$ case, $\gamma = 0$.
Values in parentheses are from Eq. (4.15).

$\beta \backslash c$	0.1	0.3	0.5	0.7	0.9	0.999
5	0	0	0	0	1.0324	1.1977
10	3.4051	3.5280	3.5469	3.4741	3.3175	3.2118
20	7.1852	6.9278	6.6489	6.3514	6.0406	5.8841
50	12.751 (12.94)	12.383 (12.54)	12.016 (12.14)	11.651 (11.74)	11.289 (11.34)	11.112 (11.14)
100	18.686 (18.80)	18.302 (18.40)	17.920 (18.00)	17.542 (17.60)	17.166 (17.20)	16.981 (17.00)
200	27.01 (27.08)	26.62 (26.68)	26.23 (26.28)	25.85 (25.88)	25.46 (25.48)	25.27 (25.29)

Table 2d. Base moment M_0 for $m = 1$, $n = 1$ case, $\gamma = 0$.
Values in parentheses are from Eq. (4.15).

$\beta \backslash c$	0.1	0.3	0.5	0.7	0.9	0.999
10	2.7980	1.3711	0	0	0	0
20	6.8875	5.9784	4.9178	3.5393	0	0
50	12.414 (12.63)	11.311 (11.56)	10.101 (10.41)	8.7289 (9.16)	7.0452 (7.77)	5.9419 (7.01)
100	18.215 (18.34)	16.820 (16.96)	15.312 (15.49)	13.648 (13.89)	11.739 (12.11)	10.636 (11.15)
200	26.33 (26.42)	24.51 (26.60)	22.55 (22.66)	20.42 (20.57)	18.03 (18.26)	16.71 (17.01)

The abridged results for different inclination angles γ are given in Table 3.

Table 3a. Base moment M_0 for $m = 4$, $n = 2$ case.
Values in parentheses are from Eq. (4.15).

γ	$\pi/4$			$\pi/2$			$3\pi/4$		
$\beta \backslash c$	0.1	0.5	0.9	0.1	0.5	0.9	0.1	0.5	0.9
10	3.9633	2.0848	0.8416	3.3630	1.9990	0.9894	1.8925	1.1762	0.6268
20	6.5824	3.9145	1.8019	5.2584	3.3787	1.8492	2.8992	1.9223	1.1181
50	11.312 (11.41)	7.5682 (7.50)	4.2981 (3.74)	8.8297 (8.88)	6.1592 (6.10)	3.8414 (3.47)	4.8222 (4.84)	3.4262 (3.39)	2.2167 (2.04)
100	16.496 (16.55)	11.683 (11.63)	7.4035 (7.03)	12.786 (12.82)	9.3059 (9.26)	6.2442 (5.99)	6.9613 (6.97)	5.1293 (5.11)	3.5252 (3.40)
200	23.79 (23.83)	17.51 (17.48)	11.94 (11.68)	18.36 (18.38)	13.77 (13.74)	9.73 (9.55)	9.98 (9.99)	7.55 (7.53)	5.42 (5.33)

Table 3b. Base moment M_0 for $m = 3$, $n = 1$ case.
Values in parentheses are from Eq. (4.15).

γ	$\pi/4$			$\pi/2$			$3\pi/4$		
$\beta\backslash c$	0.1	0.5	0.9	0.1	0.5	0.9	0.1	0.5	0.9
10	4.2061	3.0148	1.7849	3.5300	2.6657	1.7595	1.9789	1.5264	1.0483
20	6.8887	5.2039	3.4028	5.4750	4.2949	3.0256	3.0122	2.4017	1.7417
50	11.732 (11.83)	9.4074 (9.42)	6.8396 (6.67)	9.1352 (9.19)	7.4899 (7.49)	5.6671 (5.54)	4.9836 (5.01)	4.1273 (4.12)	3.1762 (3.11)
100	17.046 (17.10)	14.102 (14.11)	10.799 (10.68)	13.192 (13.22)	11.078 (11.07)	8.7004 (8.62)	7.1771 (7.19)	6.0681 (6.06)	4.8196 (4.78)
200	24.53 (24.57)	20.73 (20.74)	16.44 (16.36)	18.91 (18.93)	16.15 (16.15)	13.02 (12.96)	10.27 (10.28)	8.82 (8.81)	7.16 (7.13)

Table 3c. Base moment M_0 for $m = 2$, $n = 0$ case.
Values in parentheses are from Eq. (4.15).

γ	$\pi/4$			$\pi/2$			$3\pi/4$		
$\beta\backslash c$	0.1	0.5	0.9	0.1	0.5	0.9	0.1	0.5	0.9
10	4.4589	4.2505	3.9670	3.7038	3.5332	3.3336	2.0687	1.9787	1.8779
20	7.2051	6.8091	6.3930	5.6992	5.4429	5.1801	3.1292	3.0036	2.8760
50	12.166 (12.26)	11.676 (11.73)	11.196 (11.19)	9.4516 (9.50)	9.1473 (9.17)	8.8499 (8.84)	5.1508 (5.17)	5.0044 (5.01)	4.8613 (4.86)
100	17.616 (17.68)	17.107 (17.14)	16.608 (16.61)	13.613 (13.65)	13.298 (13.31)	12.989 (12.98)	7.4011 (7.41)	7.2496 (7.26)	7.1011 (7.10)
200	25.29 (25.33)	24.77 (24.79)	24.26 (24.26)	19.48 (19.50)	19.16 (19.17)	18.85 (18.84)	10.58 (10.59)	10.42 (10.43)	10.27 (10.27)

Table 3d. Base moment M_0 for $m = 1$, $n = 1$ case.
Values in parentheses are from Eq. (4.15).

γ	$\pi/4$			$\pi/2$			$3\pi/4$		
$\beta\backslash c$	0.1	0.5	0.9	0.1	0.5	0.9	0.1	0.5	0.9
10	4.2420	3.1045	1.7667	3.5656	2.7942	1.8643	1.9985	1.6018	1.1234
20	6.9783	5.5486	3.6831	5.5348	4.5383	3.2950	3.0419	2.5250	1.8898
50	11.853 (11.96)	9.9434 (10.09)	7.5785 (7.87)	9.2106 (9.27)	7.8274 (7.90)	6.1519 (6.29)	5.0199 (5.05)	4.2908 (4.32)	3.4157 (3.47)
100	17.173 (17.24)	14.692 (14.78)	11.720 (11.89)	13.271 (13.31)	11.445 (11.49)	9.2810 (9.36)	7.2150 (7.23)	6.2449 (6.26)	5.1014 (5.14)
200	24.66 (24.70)	21.35 (21.41)	17.46 (17.56)	18.99 (19.02)	16.53 (16.56)	13.66 (13.71)	10.31 (10.32)	9.00 (9.01)	7.47 (7.49)

Instead of graphs, our results are given in tables to facilitate their use in practice and to show the differences between the exact numerical values and the asymptotic approximations.

6. Discussions

For the stability problem of a standing column, explicit formulas for the critical load for a pointy tip ($c = 1$) can be expressed in terms of Bessel functions. For a blunt tip, we numerically found the critical loads, which are quite sensitive to the taper c and cross sectional shapes (m, n).

Our asymptotic analysis for large β is entirely new. We are fortunate to obtain a solution up to first order. The asymptotic results compare well with numerical integration, which suffers from stiffness problems when $\beta > 100$.

The results for post buckling deformations are reflected in Tables 2 and 3. We find when the gravity parameter β increases, perhaps due to acceleration of the system, the base moment M_0 increases. Fig. 4 shows the typical post buckling shapes. Note that when β is large, the boundary layer character (of large changes in slope) is evident near the base region.
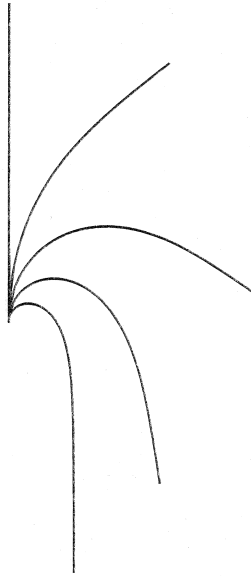

FIG. 4. Effect of gravity on deformation shape ($m = 4$, $n = 2$, $c = 0.5$, $\gamma = 0$). From top: $\beta < 12.054$, $\beta = 13$, 20, 50, 200.

In general, when the taper increases, the base moment decreases, as shown in Fig. 5. That is because there is less total weight for larger taper. However an exception is the $m = 2$, $n = 0$ cross section (Fig. 2c, along axis A-A),
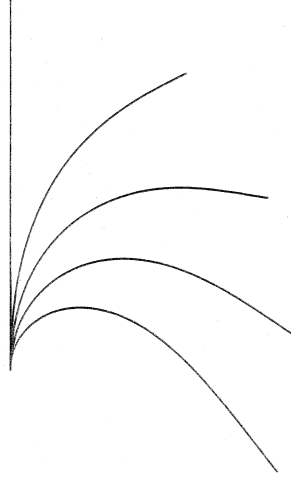
FIG. 5. Effect of taper on deformation shape (m=4, n=2, $\beta = 20$, $\gamma = 0$) From top:
$c > 0.838$, $c = 0.8$, 0.7, 0.5, 0.1.

where at low β, the effect is opposite. This cross section also behaves differently for the critical load in Table 1. Such interesting results should be investigated experimentally.

Figure 6 shows typical post buckling shapes when the base angle is varied. An increase in base angle decreases the base moment.
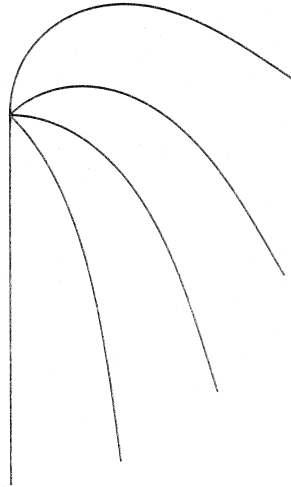

FIG. 6. Effect of base inclination ($m = 4$, $n = 2$, $c = 0.5$, $\beta = 20$) From top: $\gamma = 0$, $\pi/4$, $\pi/2$, $3\pi/4$, π.

The effect of cross sectional shape (and bending direction) is shown in Fig. 7. We cannot give a general statement on the trend, but only note that the cantilever cross section has non negligible effects of the cantilever shape.
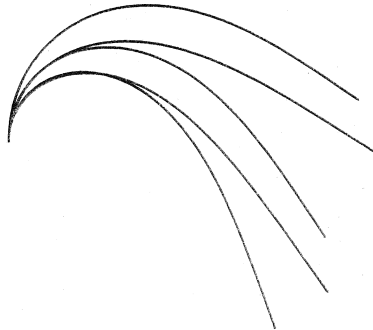
FIG. 7. Effect of cross sectional shape on deformation. (c=0.5, β=20, $\gamma = 0$) (m, n) from top: (4,2), (1,1), (3,1), (0,0), (2,0).

In conclusion, our present work greatly advances the current knowledge of heavy tapered cantilevers, especially large deformations.

References

1. L. Euler, *De Curvis Elasticis*, 1744.

2. A.G. Greenhill, *Determination of the greatest height consistent with stability that a vertical pole or mast can be made, and of the greatest height to which a tree of given proportions can grow*, Proc. Camb. Phil. Soc., **4**, 65–73, 1881.

3. W.G. Bickley, *The heavy elastica*, Phil. Mag. Ser. 7, **17**, 603–622, 1934.

4. C.Y. Wang, *Large deformations of a heavy cantilever*, Quart. Appl. Math., **39**, 261–273, 1981.

5. C.Y. Wang, *A critical review of the heavy elastica*, Int. J. Mech. Sci., **28**, 549–559, 1986.

6. S.B. Hsu, S.F. Hwang, *Analysis of large deformation of a heavy cantilever*, SIAM J. Math. Anal., **19**, 854–866, 1988.

7. T. Belendez, M. Perez-Polo, C. Neipp, A. Belendez, *Numerical and experimental analysis of large deflections of cantilever beams under a combined load*, Phys. Scrip., **T118**, 61–65, 2005.

8. P.B. Goncalves, D.L.B.R. Jurjo, C. Magluta, N. Roitman, D. Pamplona, *Large deflection behavior and stability of slender bars under self weight*, Struct. Eng. Mech., **24**, 709–725, 2006.

9. S.T. Santillan, R.H. Plaut, T.P. Witelski, L.N. Virgin, *Large oscillations of beams and columns including self-weight*, Int. J. Nonlinear Mech., **43**, 761–771, 2008.

10. A.N. Dinnik, *Buckling and Torsion*, Acad. Nauk. CCCP, Moscow 1955 [in Russian].

11. C.A. Stuart, *Buckling of a heavy tapered rod*, J. Math. Pure Appl., **80**, 281–337, 2001.

12. S.F. Hwang, L.R. Yeh, *Analysis of large deformation of a nonprismatic beam*, Taiwan. J. Math., **3**, 89–106, 1999.

13. C.A. STUART, G. VUILLAUME, *Buckling of a critically tapered rod, properties of some global branches of solutions*, Proc. Roy. Soc. London **A460**, 3261–3282, 2004.

14. P.C. RAJU, G. VENKATESWARA RAO, *Post-buckling of tapered cantilever columns*, Comp. Meth. Appl. Mech. Eng., **15**, 201–206, 1978.

15. B.K. LEE, J.F. WILSON, S.J. OH, *Elastica of cantilevered beams with variable cross sections*, Int. J. Nonlinear Mech., **28**, 579–589, 1993.

16. B.P. MADHUSUDAN, V.R. RAJEEV, B. NAGESWARA RAO, *Post-buckling of cantilever columns having variable cross-section under a combined load*, Int. J. Nonlinear Mech., **38**, 1513–1522, 2003.

17. G.M. MURPHY, *Ordinary Differential Equations and Their Solutions*, Van Nostrand, Princeton, New Jersey, 1960.